Wildfire Severity Zoning Through Google Earth Engine and Fire Risk Assessment: Application of Data Mining and Fuzzy Multi-Criteria Evaluation in Zagros Forests, Iran

Hamed Heidari (hamed_heydari70@yahoo.com)
Shool of Environment, College of Engineering, Unersity of Tehran https://orcid.org/0000-0002-7228-9304

Mostafa Keshtkar
Shahid Beheshti University

Niloofar Moazzeni
Shahid Beheshti University

Meisam Jafari
Islamic Azad University Najafabad Branch

Hossein Azadi
Department of Gheography, Ghent University, Ghent, Belgium

Research Article

Keywords: Burn severity, Fire risk assessment, Plant Species Diversity, Multi-Objective Land Allocation, Remote sensing, Google earth engine

Posted Date: March 5th, 2021

DOI: https://doi.org/10.21203/rs.3.rs-268484/v1

Abstract

The arid and semi-arid regions of Zagros forests in the Middle East are constantly exposed to wildfire due to ecological conditions, and support systems are inefficient in controlling wildfires due to managerial and social weaknesses. Remote sensing and assessment tools are suitable for rapid prevention and action to identify the severity and location of a wildfire. This study investigated the natural resource management of Zagros Forestry in terms of protecting wildfire and combating forest wildfires using the NASA fire spatial data and the wildfire severity in the Google Earth Engine (GEE) platform. The land-use of the study area is produced by applying the Random Forest (RF) classification method and data from the Sentinel 2 satellite imagery for 2019. To separate the types of cultivation and vegetation of the region, the method of extracting the average vegetation index of the seasons is extracted from GEE. To evaluate fire risk, eleven human and ecological factors and two assessment models are applied to classify the probability fire risk therein. Furthermore, the outcome of AUC confirmed the Logistic Regression (LR) model; the accuracy of the LR (AUC=0.875049) model is satisfactory and is suitable for fire risk mapping in Zagros Forestry. Six high-risk areas of the wildfire were identified by MOLA, which overlap with protected areas. Out of a total of 20469.17 Ha of wildfire, 10426.41 Ha belong to these protected areas. 3826 Ha of this area were in the forests of Amygdalus spp, Quercus brant ii, pistacia Atlantica, and Quercus Infectoria, and 6600.41 Ha of it were in rangelands. Accordingly, an executive order was developed for the decision support system that reduces the risk of wildfire and helps extinguish the wildfire.

1. Introduction

Forests are the main natural resources and are an indicator of the prevailing ecological situation in the area. Forest ecosystems are constantly changing. These changes can be due to human development or part of the evolution of nature itself (Dimopoulou and Giannikos, 2001). The considerable damages due to wildfires are directed to the environment, human health, and property (GS, 2003). Wildfire as the most important disturbing factor in ecosystems leads to the most dramatic changes in the structure and function of forest (González-Pérez et al., 2004). The degree of degradation of the ecosystem and its function due to wildfires as opposed to landscapes as differences in the severity of wildfires from local to regional scales, and this wildfire-induced ecological change, is a major focus of many studies worldwide (Naderpour et al., 2019; Parks et al., 2014). These studies often depend on network metrics that pre- and post-fire images use to estimate the rate of change caused by fire, and the most common matrix is the normal delta burn ratio, which is used to calculate dNBR, RdNBR, and RBR, and for large processing, it is better to use GEE (Key and Benson, 2006). There exist many different methods and models involved in evaluating forest fire risk (FFR) in different areas at different scales and different efficiencies. In some studies, the Dong model is applied in predicting high-risk fire areas in the forests (XU et al., 2005; E et al., 2004; Eskandari et al., 2013), and in some, the Analytic Hierarchy Process (AHP) or fuzzy sets are applied in modeling FFR (Chuvieco and Congalton, 1989; Vadrevu et al., 2010; Sowmya and Somashekar, 2010; A et al., 2012).

The forest wildfire process is typical, nonlinear, and complex, and it is influenced by many ecological and human factors. This fact, in turn, makes the task of seeking high accuracy prediction modes difficult (Pettinari and Chuvieco, 2017). In the research that has been done in this regard, Ngoc-Thach, Nguyen et al. (2018) ran a study where the advanced machine learning models like Support Vector Machine classifier (SVMC), Random Forest (RF), and Multilayer Perceptron Neural Network (MLP-Net) were applied. They, first, established a GIS database of 564 forest fire locations and then considered ten variables for the study area. Next, they applied the Pearson correlation method in assessing the correlation between variables and forest fire and then applied the MLP-Net model (Pourghasemi et al., 2020). Using three machine learning algorithms, satellite imagery, and ten influential factors, they have modeled, predicted, and evaluated the accuracy of the models in South Zagros (Nami et al., 2018a). By analyzing spatial patterns and five tree-based classifications, decision making includes alternating decision tree (ADT), classification and regression tree (CART) (Gayen and Pourghasemi, 2019), functional tree (FT), logistic model tree (LMT) (Kim et al., 2018), and Naïve Bayes tree (NBT) for wildfire pattern, and the ADT classifier performed best (Jaafari and Pourghasemi, 2019)

The Frequency Ratio (FR) and AHP models are applied for FFR mapping in a comparative study run on Melghat Tiger Reserve forest, central India by Kayet et al. (2020); the results obtained from applying FR and AHP indicate that though the trends were similar, FR model has significantly higher accuracy compared with the AHP.

For predicting the spatial pattern of fire risks even now, the Neural Network (NN) (Cheng and Wang, 2008; Satir et al., 2016), SVM (Sakr et al., 2011), RF (Arpaci et al., 2014; Oliveira et al., 2012), the Logistic Regression (LR) classifier kernel function (Tien Bui et al., 2016), and MCE fuzzy (Tien Bui et al., 2017) machine learning approaches are being applied.

According to studies on wildfire assessment and modeling, researchers have only been looking for a way to assess wildfire and compare their methods, the results of which only examine the accuracy of the models. In the present study, there is an accurate method of extracting the burnt area where the wildfire severity was estimated, and by applying the normalized difference vegetation index of Landsat satellite imagery, before and after, the wildfire is discussed in Google Earth Engine platform (Parks et al., 2018). Using MCE fuzzy (Eskandari and Miesel, 2017; Kahraman et al., 2014) and LR (Pourtaghi et al., 2016; Were et al., 2015; Satir et al., 2016), wildfire and risk zoning is done (Guo et al., 2016). Multi-Objective Land Allocation (MOLA) (Canova, 2006) was used to identify high-risk areas, investigate the extent of plant species degradation, and provide management strategies to combat and prevent wildfire. Assuming that satellite images and spatial data can be used to extract the severity and risk of wildfire, using the final risk map, it is possible to extract high-risk areas of wildfire according to the history of the wildfire and the importance of the area. Which machine learning method offers better decision making?

How can potential protection zones be extracted using decision support methods?

2. Methods And Materials

2.1. Study area

The study zone is the Zagros Mountain chain in West Iran (at 46 ° 28' N to 46 ° 22' N and 45 ° 52' E to 47 ° 58' E), one of the sub-basins of the western rivers, which is covering 1342387.14 Ha (Fig.1). The climate there is semi-arid and Mediterranean with a temperature average of 15.6 °C. The annual precipitation mean is 503 mm (Table 1). The vegetation is of semi-arid type in the sparse distribution of trees and short weed and grass (Sadeghifar et al., 2020). From 2012 to 2019, 622 wildfires are recorded in 1840 points in the wildfire information resource management system in the study zone (NASA FIRMS, 2019[1]).

In this study, according to the set goals, questions, and hypotheses, the conceptual framework was designed in 6 stages according to Fig. 2. In the first step, information was collected from responsible sources and organizations. The second step is to process the information received or extract the information. In the third step, LR and fuzzy MCE, Wildfire zoning models were performed and then the models were evaluated in the next step. The fifth step was to assess the risk of wildfire with selected model. Step six is to select high-risk locations and develop management scenarios.

2.2. Data analysis

2.2.1. Data gathering

Identification of factors involved in forest wildfire is essential in constructing a model to assess its fire risk. In this study, these factors are extracted from the available studies and the formal reports of the local state authorities. In general, forest wildfire has to do with the climatic conditions, vegetation dryness, zone topography, and human activities (Eskandari, 2017; Hong et al., 2017; Valdez et al., 2017). The NDVI, slope, aspect, and land use constitute the important variables necessary to be addressed in evaluating the fire risk (Nami et al., 2018b; Parisien et al., 2012). Moreover, the data on land cover and human accessibility are contributive to the analyzing process, because human is influential in the spatial setup and the frequency of forest wildfire. By manipulating nature in this case, humans make natural vegetation vulnerable to wildfire occurrences (Parisien et al., 2016). Accordingly, eleven parameters influence forest wildfire: slope (%), NDVI, wind speed (km/h), precipitation (mm), temperature (°C), land use specification, distance from road (m), distance from cities (m), distance from villages (m), aspect, and Mean Sea Level (MSL) (m) (Fig.6). For NDVI and land use, these factors are measured through the GEE. For a more detailed survey of vegetation and land use, in this article, the NDVI is calculated in two ways: 1) the last growing season of the study area (Rouse et al., 1974) (Fig. 4) and 2) the variations in vegetation coverage. The average NDVI of four seasons in the region is calculated and extracted as the NDVI of the seasons (Link) (Fig. 3). Consequently, the types of vegetation that have grown in the area over a year can be identified. This method can be adapted to identify and classify the type of cultivation and vegetation segregation. To calculate land use, the Sentinel 2 satellite imagery, NDVI seasons, and Landsat Urban product in GEE are applied (Pesaresi et al., 2015). All the data in this study are extracted at 30 meters resolution. The land-use consists of six factors including forests, water, bare land, grassland, and urban and agricultural classes, which are obtained through the RF algorithm (Li et al., 2020) (Link) (Fig. 5).

Table 1. Data Resource Description Table

Data	The extracted and produced annual data		Scale	Data source extraction
	Extracted	Processed and Produced		
Sentinel 2C	2019	-	10 m	European Union/ESA/Copernicus
Landsat 8	2019	-	30 m	USGS
Global Human Settlement Layers, Built-Up Grid	2019	-	38 m	EC JRC
Digital elevation models (Aster)	2010	-	30 m	ASF
Land cover type	2018	-	1:250000	FRWMO
Wildfire severity range	-	2019	10 m	GEE & UNOOSA
Seasonal and annual mean NDVI	-	2019	10 m	GEE
Land use	-	2019	30 m	GEE
Wildfire information	2012-19	-	-	FIRMS

Note: The data on climate are extracted in 2019 from IRIMO (Link), the data on Road and Transportation are extracted in 2018 from MRUD (Link), the data on protected areas are extracted from the Department of Environmental Protection Agency, Iran, 2015 from DOEIR (Link).

2.3. Fire severity determined through the Google Earth Engine

Naturally, every wildfire incident has its address and time, which is recorded by the authorities. The GEE is applied to advance the speed of process. The date before and after every wildfire incident and its location are specified through Landsat and or Sentinel 2 images (Mallinis et al., 2018). The normal burn ratio (NBR) is applied in designing the highlight burned areas and estimates the severity therein (Key, 2006). The NIR and SWIR wavelengths are applied in extracting the wildfire scope. The fresh vegetation before the fire is of high NIR and low SWIR responses, while the opposite holds true in recently burned areas. NBR is measured for both pre-fire and post-fire. To obtain the difference NBR (dNBR) image (Miller and Thode, 2007), the latter is subtracted from the former (Gibson et al., 2020). According to Veraverbeke et al. (2010), dNBR is applied to assess burn severity, where the higher the dNBR volume, the more severe the damage, while vegetation regrowth is evident in areas with negative dNBR volumes. The dNBR can be classified according to burn severity ranges proposed by the United States Geological Survey, Table 2.

Table 2. *Burn severity classes and thresholds proposed by USGS (2019)*

Severity Level	dNBR Range (scaled 10^3)	dNBR Range (not scaled)
Enhanced Regrowth, high (post-fire)	-500 to -251	-0.500 to -0.251
Enhanced Regrowth, high (post-fire)	-250 to -101	-0.250 to -0.101
Unburned	-100 to +99	-0.100 to +0.99
Low Severity	+100 to +269	+0.100 to +0.269
Moderate-low Severity	+270 to +439	+0.270 to +0.439
Miderate-high Severity	+440 to +659	+0.440 to +0.659
High Severity	+660 to +1300	+0.660 to +0.1300

The mathematical interpretation of Table 2 content is expressed through Eq. (1) introduced by Keeley (2009) and Eqs. (2) and (3) introduced by Gibson et al. (2020) as follows:

dNBR or ΔNBR = PrefireNBR – PostfireNBR

$$\text{dNBR or } \Delta\text{NBR} = \text{PrefireNBR} - \text{PostfireNBR} \quad (1)$$

$$\text{PreNBR} = \left(\frac{pre\ NIR - pre\ SWIR}{pre\ NIR + pre\ SWIR}\right) \quad (2)$$

$$\text{PostNBR} = \left(\frac{\text{Post } NIR - \text{Post } SWIR}{\text{Post } NIR + \text{Post } SWIR}\right) \qquad \text{dNBR} = \text{PreNBR} - \text{postNBR} \quad (3)$$

The Ranges of all identified wildfires are extracted from GEE through a sample code provided by the United Nations for space disaster management and emergency response (UNOOSA 2019[1]). This code is defined for both Landsat 8 and sentinel 2 images and is applied as needed (Fig. 7) (Link).

2.4. Analysis

2.4.1. Random Forest classification

The Random Forests (RF) classifier is a machine learning technique proposed by Breiman (BREIMAN, 2001), widely applied for classifying, regressing, and evaluating input factors with relative importance (Yu et al., 2017). The RF is an ensemble of learning approaches where a set of decision tree classifiers are developed to make prediction(s) (Belgiu and Drăguţ, 2016).. Consequently, different sub-datasets are generated by replacing the training dataset in a random manner, where each sub-dataset is applied in constructing a decision tree by the Classification And Regression Tree (CART) algorithm (Breiman and Friedman, 1984).

2.4.2. Logistic Regression (LR) Analysis

This analysis is frequently applied for prediction and explanation of the caused fire by humans. The binomial logistic is performed through this regression. In this process, the input dependent variable must be binary in nature, with possible values of 0 and 1. The LR analysis is usually applied to estimate a model describing the correlation among one or more continuous independent variable(s) and the binary dependent variable. In this study, LR analysis was performed using TerrSet software 18.07. Parameters used in the model: slope (%), NDVI, wind speed (km/h), precipitation (mm), temperature (°C), land use specification, distance from road (m), distance from cities (m), distance from villages (m), aspect, and Mean Sea Level (MSL) (m).

2.4.3. Fuzzy Multi-Criteria Evaluation (MCE)

MCE is a decision support tool, based on the criterion. The basis for a decision is known as a criterion. By applying MCE, it is sought to make a combination of criteria to find a single composite basis for a decision, with a specific objective orientation. In this context, these developed criteria might be variables like proximity to roads, slope, exclusion of reserved lands, etc. The appropriate images may be combined with the MCE to form a single proper map from which the final choice will be made (Bonissone and Decker, 1986).

These criteria may combine both the weighted factors and constraints. Each one of the fuzzy evaluation factors is within 1 to 255 range. The Weighted Linear Combination (WLC) is obtained by multiplying each one of the evaluation factors in AHP weight derivatives. To obtain the relative weight of each factor in the multi-criteria evaluation, the AHP weighting method is applied. The AHP weighing table was applied to this model after completing a questionnaire provided to ecologists, forestry experts, managers of environment, and natural resources. The most effective Wildfire weights for NDVI were land use specification and wind speed. To assess the stability of AHP weights it CR, should be measured. If this rate < 0.1, the validated is acceptable. In this study, the obtained CR is 0.07, an acceptable one. The CR consistency index is calculated through Eqs. (4) and (5),(Finan and Hurley, 1997):

$$CI = \frac{\lambda_{max} - n}{n - 1} \quad (4)$$

$$CR = \frac{CI}{RI} \quad (5)$$

Where, CI is the compatibility index pairwise comparison matrix, CR is the consistency rate, λ_{max} is the maximum eigenvalue judgment matrix, RI is the random index and n is the compared components' count in the matrix (Ergu et al., 2011).

2.4.4. Models validation

Relative operating characteristics (ROC) are applied to validate the evaluation models, which are proper in assessing the validity of a model that predicts the location of the occurrence of a class by choosing an appropriate image for depicting the likelihood of that class occurrence.

AUC volume is applied to calculate the Area Under the Curve (Pontius Jr and Batchu, 2003), which is constitute the output of ROC. AUC value at 1 indicates that there is a perfect spatial agreement between the class map (range of fire severity produced from GEE) and the appropriateness map (models output). An AUC volume of higher than 0.5 is acceptable for model validation (Gilmore Pontius and Pacheco, 2004).

2.4.5. Multi-Objective Land Allocation (MOLA)

MOLA is a procedure for solving single and multiple objective land allocation problems. As to multi-objective land allocation problems, a compromised solution, according to the data extracted from a set of appropriate maps, is determined by MOLA, for each objective. This solution would optimize land appropriateness for each objective, according to the assigned weights, therein. To solve the allocation problem, the user can specify either the area or maximum budget requirements. There exist options to force contiguity and compactness. The suitability maps are usually extracted from MCE. The single objective of land allocation procedure of MOLA is to solve a single-objective allocation problem. Based on the information from a single objective, or appropriateness map, the best solution given the specified constraints is determined. For both procedures, the user can specify spatial objectives like contiguity and compactness, non-spatial constraints like areal requirements for the objective, and maximum budget requirement based on the land price. In this study, the fire risk map obtained from the logistic regression analysis method and the average models method as the base input is fed into the single objective land allocation method by applying the TerrSet s/w. For the final location and protection prioritization, according to the maximum fire in the area, the proper area is calculated and assigned. In this study, three spatial sites are applied to logistic regression analysis and average models. The spatial sites are prioritized based on the highest value of map pixels, according to the spatial location of protected areas and the type of coverage, under the Environment Organization's supervision.

3. Results

3.1. Wildfire severity

The range of all wildfires was extracted from 2012 to 2019 using GEE, as shown in Table 3.

Table 3. Classes and information of burned areas from 2012 to 2019

Class name	(Ha)	(%)
Low severity	14115.78	68.96
Moderate Low Severity	5645.88	27.58
Miderate High Severity	701.64	3.43
High Severity	5.85	0.03
	20469.15	100

Class of burned areas	Area(Ha)	Perecent(%)
Low severity	14115.78	68.96
Moderate Low Severity	5645.88	27.58
Miderate High Severity	701.64	3.43
High Severity	5.85	0.03
	20469.15	100

3.2. Wildfire probability map

After running and analyzing the models, in the data mining method, the logistic regression analysis model with AUC = 0.875049, (Appendix 1) and Fuzzy multi-criteria evaluation model with AUC = 0.584645 (Appendix 1) were obtained. The MCE model was rejected due to low AUC. To create a wildfire probability map, LR model wAS classified using the natural-break classification method. Fig. 8 shows the percentage of the class area of probability wildfire in each model. In the LR and MCE models, most of the areas are related to the Moderate- high severity class.

Furthermore, by comparing the class of wildfire severity in burned areas with the classes of evaluation models, it is shown that the highest area and wildfire occurred on the Low severity class (Fig. 9).

3.3. Fire risk maps

A risk map from the LR model was produced, which had the highest AUC. Then, using the number of wildfires and the point density command in Arc GIS software, the wildfire density map was created as a fire severity map. By multiplying the LR model by wildfire severity, a fire risk map is produced. The fire risk map is classified as High Risk, Miderate-high Risk, Moderate-low Risk, and Low Risk (Fig. 10).

The area of fire risk classes is shown in Fig. 11. Using the number of wildfires, the percentage occurrence of wildfires was assessed according to Fig. 12, with the highest number of wildfires occurring on the Low-risk class. Due to the high area of this class compared to the density of the number of wildfires, the risk is low. However, in both models, the high-risk class was less than 15%, and the risk of wildfire is high due to the low area and high density of the wildfire.

3.4. Selection of high-risk areas using MOLA

To identify the area's vulnerability to wildfire and propose decision making and managerial procedures, given the largest area burned in recent wildfires and using fire risk map, six areas were selected by the MOLA model as high-risk areas (Fig. 13). The proposed areas are in the vicinity areas such as Kosalan, Bozin, and Marakhil Touran which protected zones by the environmental protection agency (Table 1). So here, there are a variety of animals and protected species that will be at risk of death during a wildfire. By examining the buffer at a distance of 10 km from these areas, it was determined that out of a total of

20469.17 Ha of wildfire, 10426.41 Ha belong to these areas. This indicates that 50% of wildfires have occurred in this area (Fig. 14). The proposed areas were evaluated according to environmental factors and were classified as moderate-low value, miderate-high value, high value, and very high value in terms of protection importance.

3.5. Destruction rate of vegetation

To assess the vegetation type of burned areas using GIS data from Forests, Range, and Watershed Management Organization, Table 1, the extent of vegetation degradation in forest and rangeland species was investigated.

3.5.1. Forest species

The total area of forests in the study area is 166808 hectares, of which 6,264 hectares were burned in wildfires between 2012 and 2019, and the details are shown in Fig. 15.

By assessing the distance of 10 km from the protected areas, it was determined that the total area of forests in this area is about 74,000 hectares, of which 3826 hectares were burned in wildfires between 2012 and 2019, and the details are shown in Fig. 16.

3.5.2. Rangeland species

The land cover of the study area contains scattered forests with dense rangelands background and 13 species. The rangelands area is 408233 hectares, of which 10136 hectares were burned in wildfires between 2012 and 2019, and the details are shown in Fig. 17.

Rangelands area in 10 km of protected areas is about 107857 hectares, of which 3285 hectares were burned between 2012 and 2019, and the details are shown in Fig. 18.

4. Discussion

In this study, we have tried to develop fire risk assessment models and wildfire probability zoning, and also help improve the natural resource management process by bringing the results closer to reality. By resorting to the documents and data available in domestic and international organizations and applying remote sensing techniques together with the algorithms available in GEE and satellite images of high spatial distinction ability this assessment is accomplished. The effective features in this context are selected carefully and are weighted. Among the available methods and classification techniques, the most valid and accurate ones are applied in evaluating the potential risks in wildfire occurrence. The strong point of this study in relation to its counterparts consists of 1) applying the GEE platform with a vast supportive data, high processing speed, reduced human error coefficient, and accuracy in results and 2) applying accurate evaluating and location detecting methods, multi-criteria evaluation, and neural network. High-risk wildfire is overlapping with protected areas under the support of the Environment Organization (Kozlan, Bozin, and Marakhil Turan), and 50% of all wildfires have occurred within a 10-

kilometer range of these areas. These areas include forest species such as Amygdalus spp, Quercus brant ii, Pistacia Atlantica, Quercus Infectoria, and pastures (Grasses, Forbs, Astragalus, Acantholimon, Psathyrostachys, and Daphne) and animal species such as 117 species of birds, 23 mammals, and 17 species of reptiles. Furthermore, by examining the type of vegetation in the whole region, the burned areas, and the protected areas, it was determined separately which of the plant and forest species are endangered.

Due to the existence of Quercus forests in this region, restrictions on human non-presence in the last few decades have led to the accumulation of a high volume of dry weed and grass, i.e., high potential to wildfire occurrence. According to the obtained results, in order to accurately assess the probability and risk of wildfire, it is necessary to carefully examine the natural and human factors in the wildfire and use wildfire zones to introduce the wildfire sample to the evaluation models and it is recommended to have serious controlling measures here like in-situ wildfire extinguishing services, watchtowers, etc. In addition to online intelligent wildfire sensors, communication stations and properly designed over ground connecting networks/paths are recommended. Given that in recent wildfires, a number of volunteer firefighters have been killed, staff-training, modern equipment, aerial wildfire extinguishing equipment like helicopters, and artificial water reservoirs-resources constitute the major components in this context. Training the neighboring rural and urban population and wildlife tourist guides can be a preventive measure in wildfire occurrence prevention. In a similar study, Halofsky et al. (2020) assessed the wildfires in the NW Pacific Ocean forests with respect to climate change and found that they occur due to warming and humidity reduction in weather. Naderpour et al. (2019) recommend planting trees in colder and more humid micro-sites to protect species on the verge of extinction. Combined methods based on GIS to model forest wildfire and their classification into statistical data-oriented models yield more accurate results. Among these, the data-oriented methods are the most common methods (Parks et al., 2018). Pourghasemi et al. (2020) introduced land use, precipitation, and slop as the criteria in wildfire intensity according to Landsat to extract the dNBR, RdNBR, and RBR, which can be practical in evaluating wildfire. Hajehforooshnia et al. (2011) and Parks et al. (2014) used multi-objective land allocation (MOLA) to identify priorities and sensitive areas for the shelter during a study to expand the Qomishlu Wildlife Sanctuary.

5. Conclusion

The results of this study indicate that 12% of the study area is forest and 30% is rangelands. 1.52% of the total study area is affected by wildfire, which includes 3.7% of forests and 2.5% of rangelands. According to the objectives of this study, the risk assessment model was selected according to the AUC coefficient, and high fire risk areas were identified using the MOLA model. Due to the overlap of MOLA results with protected areas, these areas were selected as hotspot wildfires, accounting for 47% of forests and 26.42% of the region's rangelands, and 50% of all wildfires in the region have occurred in and around these areas, which is an answer to the assumptions and questions of the present study. Given that the protected areas are exactly on the border between Iran and Iraq, the choice of high-risk areas of wildfire as a firefighting base could cover the protection of forests and rangelands internationally. One of the limitations of this

study and similar studies at the time of the wildfire, in order to extract the fire zone, is the time interval of at least 15 days that we have to wait to receive satellite images after the wildfire. With the method presented in this study, researchers can assess the extent and severity of wildfires in the shortest possible time on a large scale. In addition, the online decision support system can be developed for use on a variety of scales and times.

References

A, M., SR, F. S. & R, N. 2012. Forests and rangelands' wildfire risk zoning using GIS and AHP techniques. Caspian Journal of Environmental Sciences, 43–52.

ABDEL-RAHMAN, E. M., MUTANGA, O., ADAM, E. & ISMAIL, R. 2014. Detecting Sirex noctilio grey-attacked and lightning-struck pine trees using airborne hyperspectral data, random forest and support vector machines classifiers. ISPRS Journal of Photogrammetry and Remote Sensing, 88, 48-59.

ARPACI, A., MALOWERSCHNIG, B., SASS, O. & VACIK, H. 2014. Using multi variate data mining techniques for estimating fire susceptibility of Tyrolean forests. Applied Geography, 53, 258–270.

BELGIU, M. & DRĂGUŢ, L. 2016. Random forest in remote sensing: A review of applications and future directions. ISPRS Journal of Photogrammetry and Remote Sensing, 114, 24-31.

BONISSONE, P. P. & DECKER, K. S. 1986. Selecting Uncertainty Calculi and Granularity: An Experiment in Trading-Off Precision and Complexity* *This work was partially supported by the Defense Advanced Research Projects Agency (DARPA) contract F30602-85-C0033. Views and conclusions contained in this paper are those of the authors and should not be interpreted as representing the official opinion or policy of DARPA or the U.S. Government. In: KANAL, L. N. & LEMMER, J. F. (eds.) Machine Intelligence and Pattern Recognition. North-Holland.

BREIMAN, L. 2001. Random Forests. Machine learning, 5-32.

BREIMAN, L. & FRIEDMAN, J. 1984. Classification and regression trees.

CANOVA, L. 2006. Protected areas and landscape conservation in the Lombardy plain (northern Italy): an appraisal. Landscape and Urban Planning, 74, 102-109.

CHAPI, K., SINGH, V. P., SHIRZADI, A., SHAHABI, H., BUI, D. T., PHAM, B. T. & KHOSRAVI, K. 2017. A novel hybrid artificial intelligence approach for flood susceptibility assessment. Environmental modelling & software, 95, 229-245.

CHENG, T. & WANG, J. 2008. Integrated spatio-temporal data mining for forest fire prediction. Transactions in GIS, 12, 591-611.

CHUVIECO, E. & CONGALTON, R. G. 1989. Application of remote sensing and geographic information systems to forest fire hazard mapping. Remote Sensing of Environment, 29, 147-159.

DIMOPOULOU, M. & GIANNIKOS, I. 2001. Spatial Optimization of Resources Deployment for Forest-Fire Management. International Transactions in Operational Research, 8, 523-534.

E, E., V, K. & N, M. 2004. Forest fire risk zone mapping from satellite imagery and GIS: a case study. 20th Congress of the international society for photogrammetry and remote sensing. Istanbul.

ESKANDARI, S. 2017. A new approach for forest fire risk modeling using fuzzy AHP and GIS in Hyrcanian forests of Iran. Arabian Journal of Geosciences, 10.

ESKANDARI, S., GHADIKOLAEI, J. O., JALILVAND, H. & SARADJIAN, M. R. 2013. Detection of fire high-risk areas in northern forests of iran using dong model. World Applied Sciences Journal, 27, 770-773.

ESKANDARI, S. & MIESEL, J. R. 2017. Comparison of the fuzzy AHP method, the spatial correlation method, and the Dong model to predict the fire high-risk areas in Hyrcanian forests of Iran. Geomatics, Natural Hazards and Risk, 8, 933-949.

GAYEN, A. & POURGHASEMI, H. R. 2019. Spatial modeling of gully erosion: a new ensemble of CART and GLM data-mining algorithms. Spatial Modeling in GIS and R for Earth and Environmental Sciences. Elsevier.

GIBSON, R., DANAHER, T., HEHIR, W. & COLLINS, L. 2020. A remote sensing approach to mapping fire severity in south-eastern Australia using sentinel 2 and random forest. Remote Sensing of Environment, 240, 111702.

GILMORE PONTIUS, R. & PACHECO, P. 2004. Calibration and validation of a model of forest disturbancein the Western Ghats, India 1920–1990. GeoJournal, 61, 325-334.

GONZÁLEZ-PÉREZ, J. A., GONZÁLEZ-VILA, F. J., ALMENDROS, G. & KNICKER, H. 2004. The effect of fire on soil organic matter—a review. Environment International, 30, 855-870.

GS, R. 2003. Fire risk assessment for fire control management in Chilla forest range of Rajaji National Park Uttaranchal

GUO, F., SU, Z., WANG, G., SUN, L., LIN, F. & LIU, A. 2016. Wildfire ignition in the forests of southeast China: Identifying drivers and spatial distribution to predict wildfire likelihood. Applied Geography, 66, 12-21.

HAJEHFOROOSHNIA, S., SOFFIANIAN, A., MAHINY, A. S. & FAKHERAN, S. 2011. Multi objective land allocation (MOLA) for zoning Ghamishloo Wildlife Sanctuary in Iran. Journal for Nature Conservation, 19, 254-262.

HALOFSKY, J. E., PETERSON, D. L. & HARVEY, B. J. 2020. Changing wildfire, changing forests: the effects of climate change on fire regimes and vegetation in the Pacific Northwest, USA. Fire Ecology, 16.

HIROSE, Y., YAMASHITA, K. & HIJIYA, S. 1991. Back-propagation algorithm which varies the number of hidden units. Neural Networks, 4, 61-66.

HONG, H., NAGHIBI, S. A., DASHTPAGERDI, M. M., POURGHASEMI, H. R. & CHEN, W. 2017. A comparative assessment between linear and quadratic discriminant analyses (LDA-QDA) with frequency ratio and weights-of-evidence models for forest fire susceptibility mapping in China. Arabian Journal of Geosciences, 167.

JAAFARI, A. & POURGHASEMI, H. R. 2019. 28 - Factors Influencing Regional-Scale Wildfire Probability in Iran: An Application of Random Forest and Support Vector Machine. In: POURGHASEMI, H. R. & GOKCEOGLU, C. (eds.) Spatial Modeling in GIS and R for Earth and Environmental Sciences. Elsevier.

KAHRAMAN, C., ÖZTAYŞI, B., UÇAL SARı, İ. & TURANOĞLU, E. 2014. Fuzzy analytic hierarchy process with interval type-2 fuzzy sets. Knowledge-Based Systems, 59, 48-57.

KAYET, N., CHAKRABARTY, A., PATHAK, K., SAHOO, S., DUTTA, T. & HATAI, B. K. 2020. Comparative analysis of multi-criteria probabilistic FR and AHP models for forest fire risk (FFR) mapping in Melghat Tiger Reserve (MTR) forest. Journal of Forestry Research, 31, 565-579.

KEELEY, J. E. 2009. Fire intensity, fire severity and burn severity: A brief review and suggested usage. International Journal of Wildland Fire, 18, 116-126.

KEY, C. H. 2006. Ecological and Sampling Constraints on Defining Landscape Fire Severity. Fire Ecology, 2, 34-59.

KEY, C. H. & BENSON, N. C. 2006. Landscape assessment (LA). In FIREMON: Fire Effects Monitoring and Inventory System. USA.

KILIÇ, M. & KAYA, İ. 2015. Investment project evaluation by a decision making methodology based on type-2 fuzzy sets. Applied Soft Computing, 27, 399-410.

KIM, J.-C., LEE, S., JUNG, H.-S. & LEE, S. 2018. Landslide susceptibility mapping using random forest and boosted tree models in Pyeong-Chang, Korea. Geocarto International, 33, 1000-1015.

LEE, S. & SAMBATH, T. 2006. Landslide susceptibility mapping in the Damrei Romel area, Cambodia using frequency ratio and logistic regression models. Environmental Geology, 50, 847-855.

LEE, S. & TALIB, J. A. 2005. Probabilistic landslide susceptibility and factor effect analysis. Environmental Geology, 47, 982-990.

LI, Q., QIU, C., MA, L., SCHMITT, M. & ZHU, X. X. 2020. Mapping the land cover of africa at 10 m resolution from multi-source remote sensing data with google earth engine. Remote Sensing, 12.

MALLINIS, G., MITSOPOULOS, I. & CHRYSAFI, I. 2018. Evaluating and comparing Sentinel 2A and Landsat-8 Operational Land Imager (OLI) spectral indices for estimating fire severity in a Mediterranean pine ecosystem of Greece. GIScience & Remote Sensing, 55, 1-18.

MILLER, J. D. & THODE, A. E. 2007. Quantifying burn severity in a heterogeneous landscape with a relative version of the delta Normalized Burn Ratio (dNBR). Remote Sensing of Environment, 109, 66-80.

NADERPOUR, M., RIZEEI, H. M., KHAKZAD, N. & PRADHAN, B. 2019. Forest fire induced Natech risk assessment: A survey of geospatial technologies. Reliability Engineering & System Safety, 191, 106558.

NAMI, M., JAAFARI, A., FALLAH, M. & NABIUNI, S. 2018a. Spatial prediction of wildfire probability in the Hyrcanian ecoregion using evidential belief function model and GIS. International journal of environmental science and technology, 15, 373-384.

NAMI, M. H., JAAFARI, A., FALLAH, M. & NABIUNI, S. 2018b. Spatial prediction of wildfire probability in the Hyrcanian ecoregion using evidential belief function model and GIS. International Journal of Environmental Science and Technology, 15, 373-384.

NGOC THACH, N., BAO-TOAN NGO, D., XUAN-CANH, P., HONG-THI, N., HANG THI, B., NHAT-DUC, H. & DIEU, T. B. 2018. Spatial pattern assessment of tropical forest fire danger at Thuan Chau area (Vietnam) using GIS-based advanced machine learning algorithms: A comparative study. Ecological Informatics, 46, 74-85.

OLIVEIRA, S., OEHLER, F., SAN-MIGUEL-AYANZ, J., CAMIA, A. & PEREIRA, J. M. C. 2012. Modeling spatial patterns of fire occurrence in Mediterranean Europe using Multiple Regression and Random Forest. Forest Ecology and Management, 275, 117-129.

PARISIEN, M. A., MILLER, C., PARKS, S. A., DELANCEY, E. R., ROBINNE, F. N. & FLANNIGAN, M. D. 2016. The spatially varying influence of humans on fire probability in North America. Environmental Research Letters, 11.

PARISIEN, M. A., SNETSINGER, S., GREENBERG, J. A., NELSON, C. R., SCHOENNAGEL, T., DOBROWSKI, S. Z. & MORITZ, M. A. 2012. Spatial variability in wildfire probability across the western United States. International Journal of Wildland Fire, 21, 313-327.

PARKS, S. A., HOLSINGER, L. M., VOSS, M. A., LOEHMAN, R. A. & ROBINSON, N. P. 2018. Mean composite fire severity metrics computed with google earth engine offer improved accuracy and expanded mapping potential. Remote Sensing, 10, 879.

PARKS, S. A., PARISIEN, M. A., MILLER, C. & DOBROWSKI, S. Z. 2014. Fire activity and severity in the western US vary along proxy gradients representing fuel amount and fuel moisture. PLoS ONE, 9.

PESARESI, M., EHRILCH, D., FLORCZYK, A. J., FREIRE, S., JULEA, A., KEMPER, T., SOILLE, P. & SYRRIS, V. 2015. GHS built-up grid, derived from Landsat, multitemporal (1975, 1990, 2000, 2014). In: EUROPEAN

COMMISSION, J. R. C. J. (ed.).

PETTINARI, M. L. & CHUVIECO, E. 2017. Fire behavior simulation from global fuel and climatic information. Forests, 8.

PONTIUS JR, R. G. & BATCHU, K. 2003. Using the relative operating characteristics to quantify certainty in prediction of location of land cover change in India. Transactions in GIS, 7, 467-484.

POURGHASEMI, H. R., GAYEN, A., LASAPONARA, R. & TIEFENBACHER, J. P. 2020. Application of learning vector quantization and different machine learning techniques to assessing forest fire influence factors and spatial modelling. Environmental Research, 184.

POURTAGHI, Z. S., POURGHASEMI, H. R., ARETANO, R. & SEMERARO, T. 2016. Investigation of general indicators influencing on forest fire and its susceptibility modeling using different data mining techniques. Ecological Indicators, 64, 72-84.

ROUSE, J., HAAS, R., SCHELL, J. & DEERING, D. 1974. Monitoring Vegetation Systems in the Great Plains with ERTS, Washington, DC, USA, NASA Special Publication.

SADEGHIFAR, M., AGHA, A. B. A. & POURREZA, M. 2020. Comparing soil microbial eco-physiological and enzymatic response to fire in the semi-arid Zagros woodlands. Applied Soil Ecology, 147, 103366.

SAHOO, S., MUNUSAMY, S. B., DHAR, A., KAR, A. & RAM, P. 2017. Appraising the Accuracy of Multi-Class Frequency Ratio and Weights of Evidence Method for Delineation of Regional Groundwater Potential Zones in Canal Command System. Water Resources Management, 31, 4399-4413.

SAKR, G., ELHAJJ, I. & MITRI, G. 2011. Efficient forest fire occurrence prediction for developing countries using two weather parameters. Eng. Appl. of AI, 24, 888-894.

SATIR, O., BERBEROGLU, S. & DONMEZ, C. 2016. Mapping regional forest fire probability using artificial neural network model in a Mediterranean forest ecosystem. Geomatics, Natural Hazards and Risk, 7, 1645-1658.

SOWMYA, S. V. & SOMASHEKAR, R. K. 2010. Application of remote sensing and geographical information system in mapping forest fire risk zone at Bhadra wildlife sanctuary, India. Journal of Environmental Biology, 31, 969-974.

TIEN BUI, D., BUI, Q. T., NGUYEN, Q. P., PRADHAN, B., NAMPAK, H. & TRINH, P. T. 2017. A hybrid artificial intelligence approach using GIS-based neural-fuzzy inference system and particle swarm optimization for forest fire susceptibility modeling at a tropical area. Agricultural and Forest Meteorology, 233, 32-44.

TIEN BUI, D., LE, K.-T., NGUYEN, V., LE, H. & REVHAUG, I. 2016. Tropical Forest Fire Susceptibility Mapping at the Cat Ba National Park Area, Hai Phong City, Vietnam, Using GIS-Based Kernel Logistic Regression. Remote Sensing, 8.

VADREVU, K. P., EATURU, A. & BADARINATH, K. V. S. 2010. Fire risk evaluation using multicriteria analysis-a case study. Environmental Monitoring and Assessment, 166, 223-239.

VALDEZ, M. C., CHANG, K. T., CHEN, C. F., CHIANG, S. H. & SANTOS, J. L. 2017. Modelling the spatial variability of wildfire susceptibility in Honduras using remote sensing and geographical information systems. Geomatics, Natural Hazards and Risk, 8, 876-892.

VERAVERBEKE, S., VERSTRAETEN, W. W., LHERMITTE, S. & GOOSSENS, R. 2010. Evaluating Landsat Thematic Mapper spectral indices for estimating burn severity of the 2007 Peloponnese wildfires in Greece. International Journal of Wildland Fire, 19, 558-569.

WERE, K., BUI, D. T., DICK, O. B. & SINGH, B. R. 2015. A comparative assessment of support vector regression, artificial neural networks, and random forests for predicting and mapping soil organic carbon stocks across an Afromontane landscape. Ecological Indicators, 52, 394-403.

XU, D., D, L.-M., G-F, S., T, L. & W, H. 2005. Forest fire risk zone mapping from satellite images and GIS for Baihe Forestry Bureau, Jilin, China. Journal of Forestry Research, 169–174.

YILMAZ, I. 2007. GIS based susceptibility mapping of karst depression in gypsum: A case study from Sivas basin (Turkey). Engineering Geology, 90, 89-103.

YU, P.-S., YANG, T.-C., CHEN, S.-Y., KUO, C.-M. & TSENG, H.-W. 2017. Comparison of random forests and support vector machine for real-time radar-derived rainfall forecasting. Journal of Hydrology, 552, 92-104.

Figures

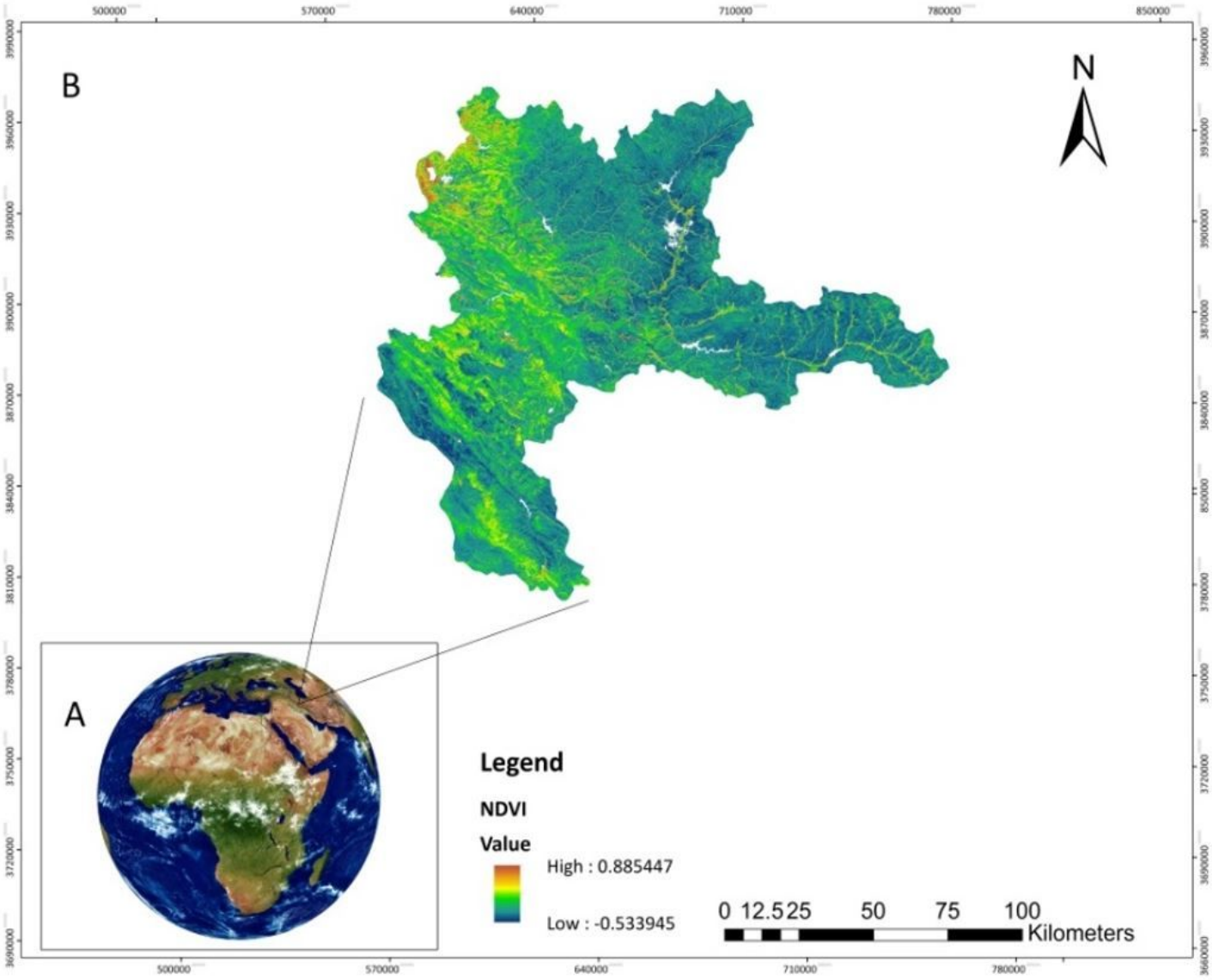

Figure 1

The location of the study area. Note: The designations employed and the presentation of the material on this map do not imply the expression of any opinion whatsoever on the part of Research Square concerning the legal status of any country, territory, city or area or of its authorities, or concerning the delimitation of its frontiers or boundaries. This map has been provided by the authors.

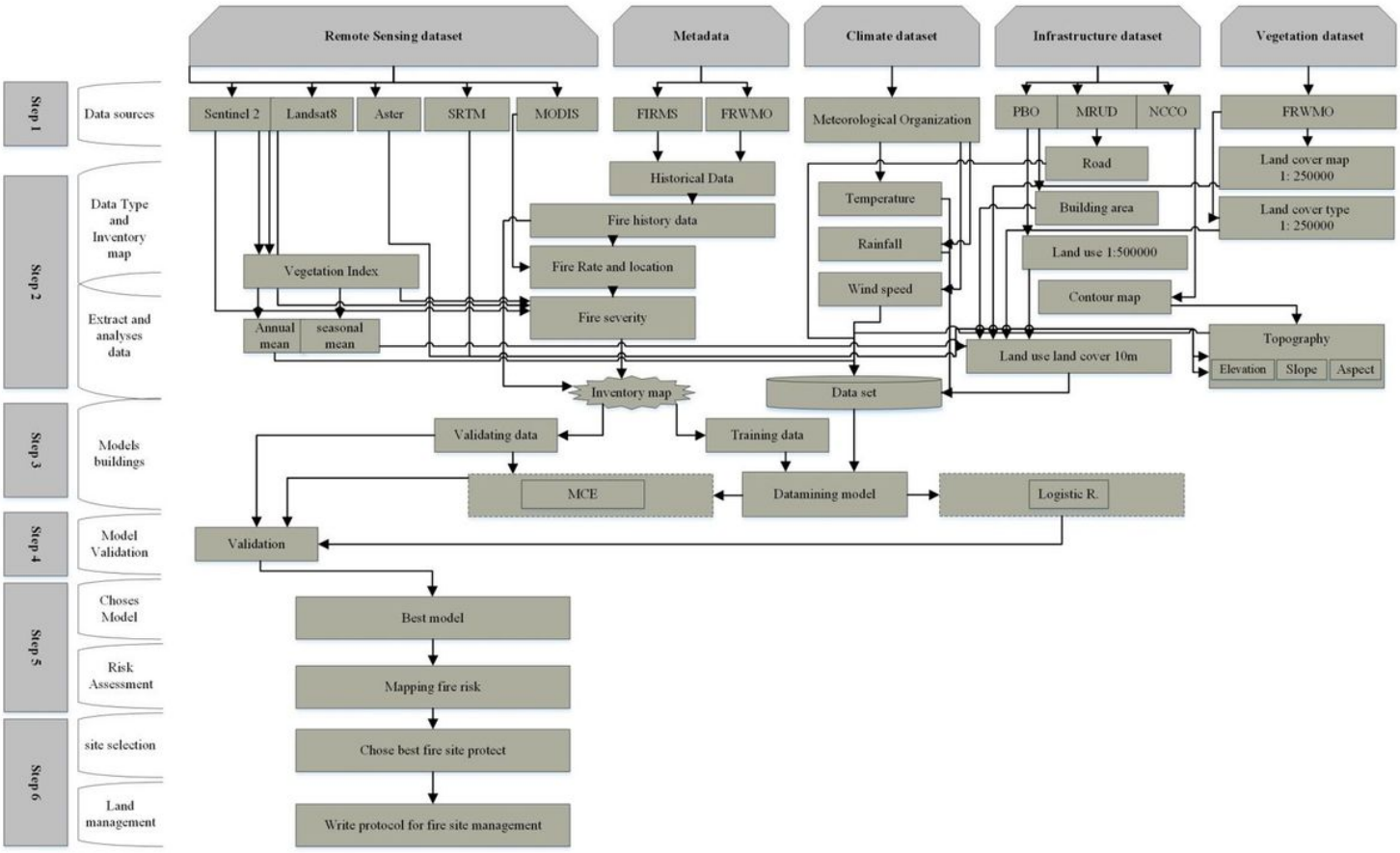

Figure 2

Methodological framework of this study for assessing fire risk maps through data mining and MCE. The flowchart is designed by the authors

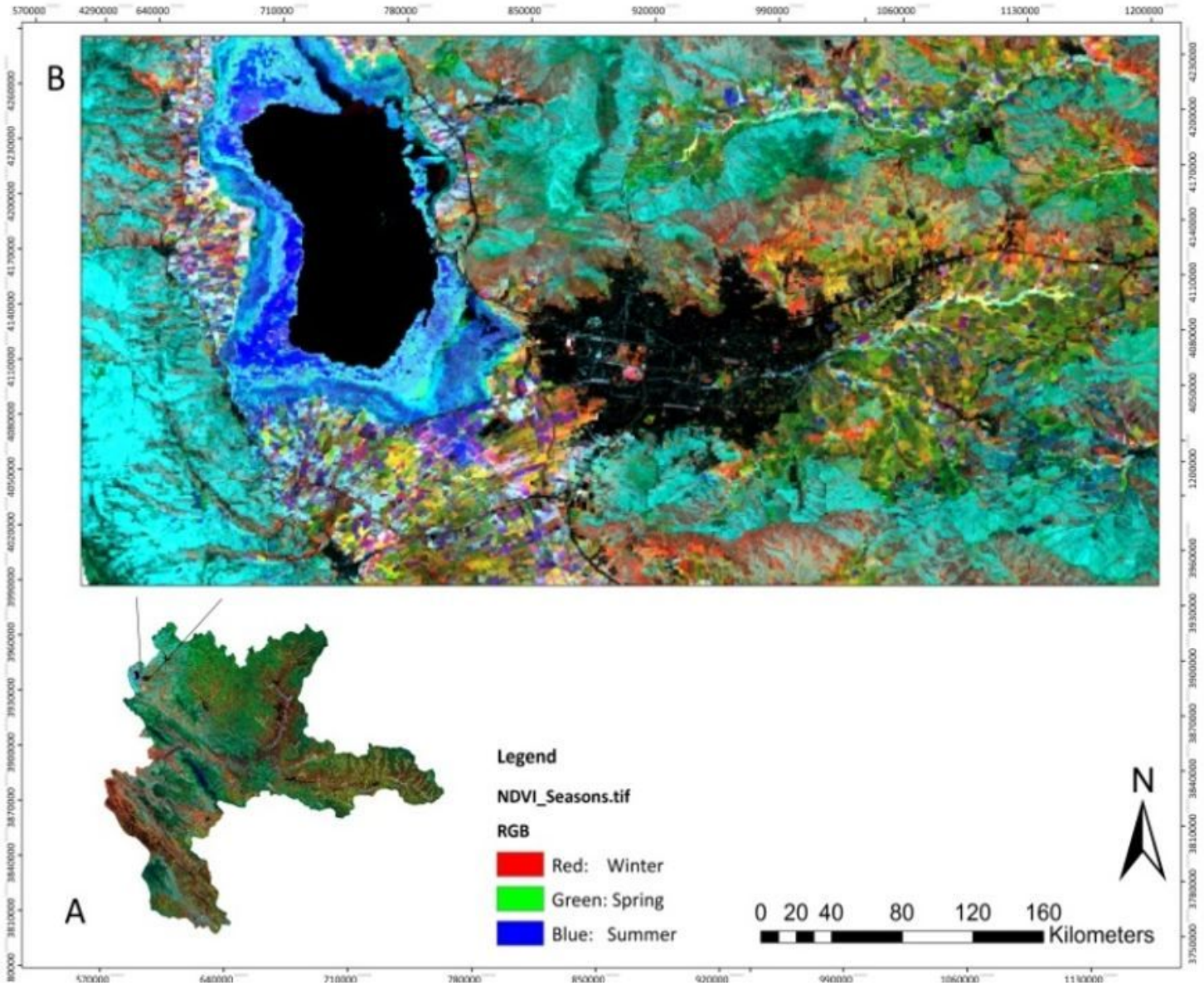

Figure 3

Average NDVI of seasons (2019). Note: The designations employed and the presentation of the material on this map do not imply the expression of any opinion whatsoever on the part of Research Square concerning the legal status of any country, territory, city or area or of its authorities, or concerning the delimitation of its frontiers or boundaries. This map has been provided by the authors.

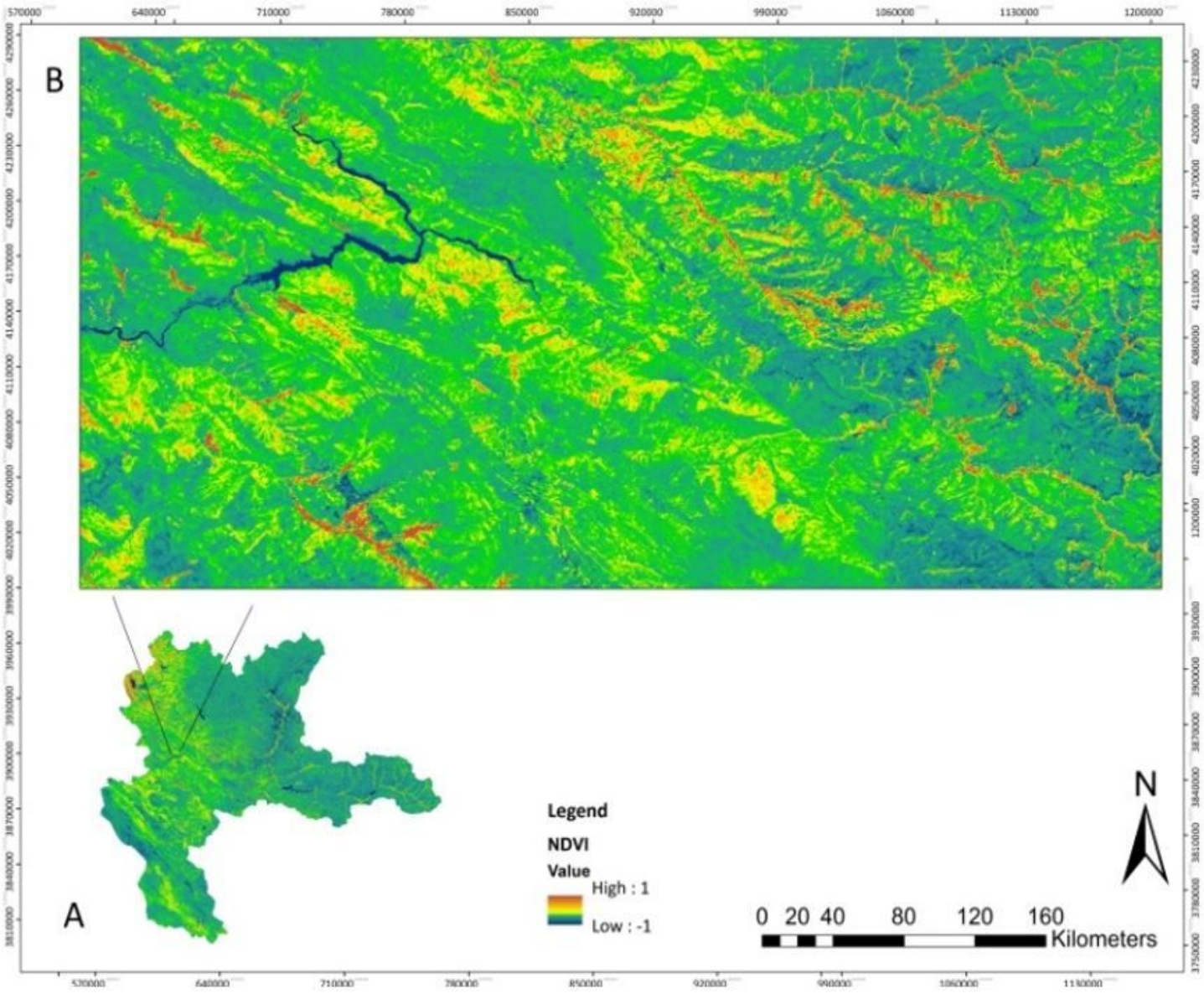

Figure 4

NDVI for summer (2019). Note: The designations employed and the presentation of the material on this map do not imply the expression of any opinion whatsoever on the part of Research Square concerning the legal status of any country, territory, city or area or of its authorities, or concerning the delimitation of its frontiers or boundaries. This map has been provided by the authors.

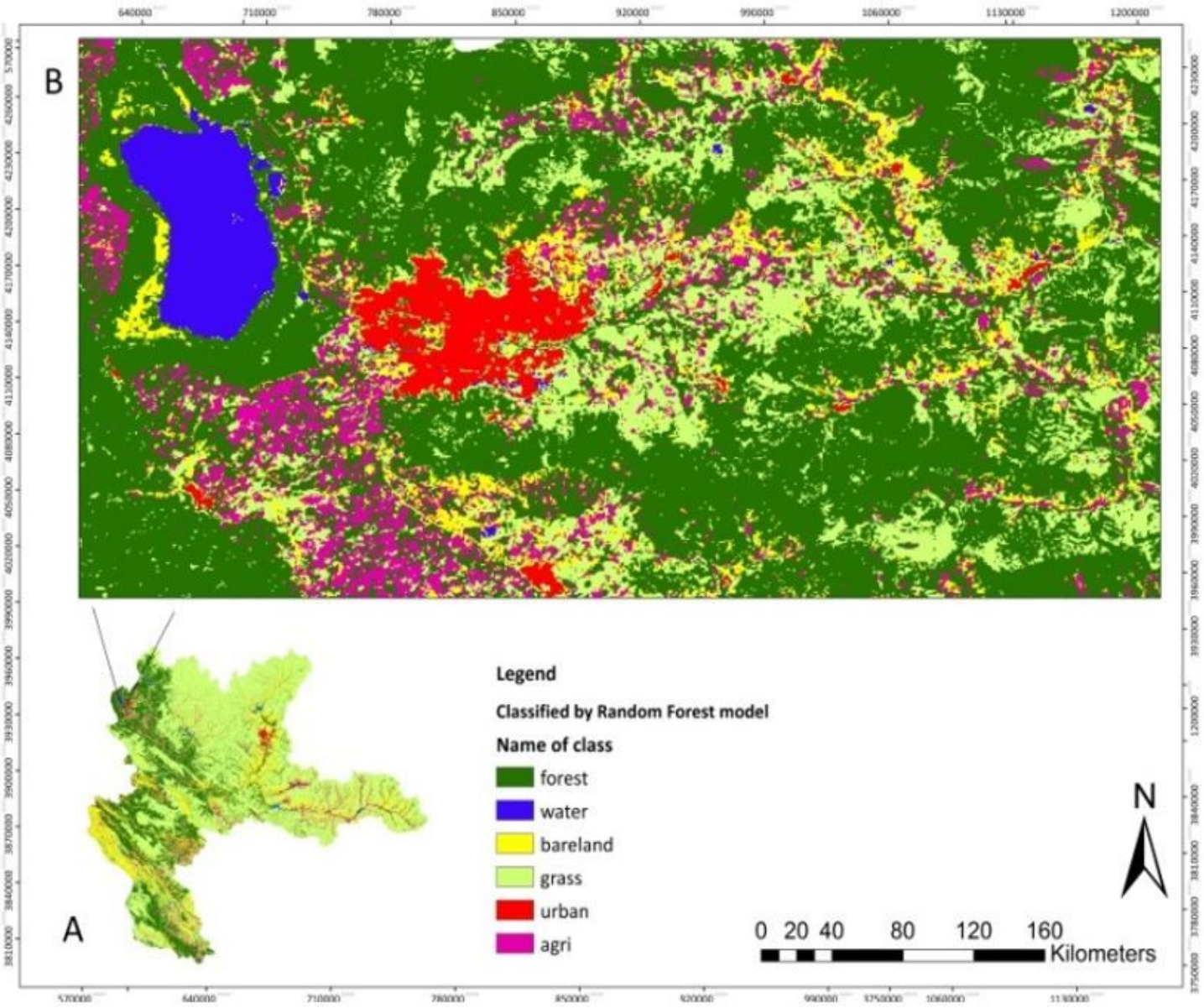

Figure 5

Land use classification using the RF method (2019). Note: The designations employed and the presentation of the material on this map do not imply the expression of any opinion whatsoever on the part of Research Square concerning the legal status of any country, territory, city or area or of its authorities, or concerning the delimitation of its frontiers or boundaries. This map has been provided by the authors.

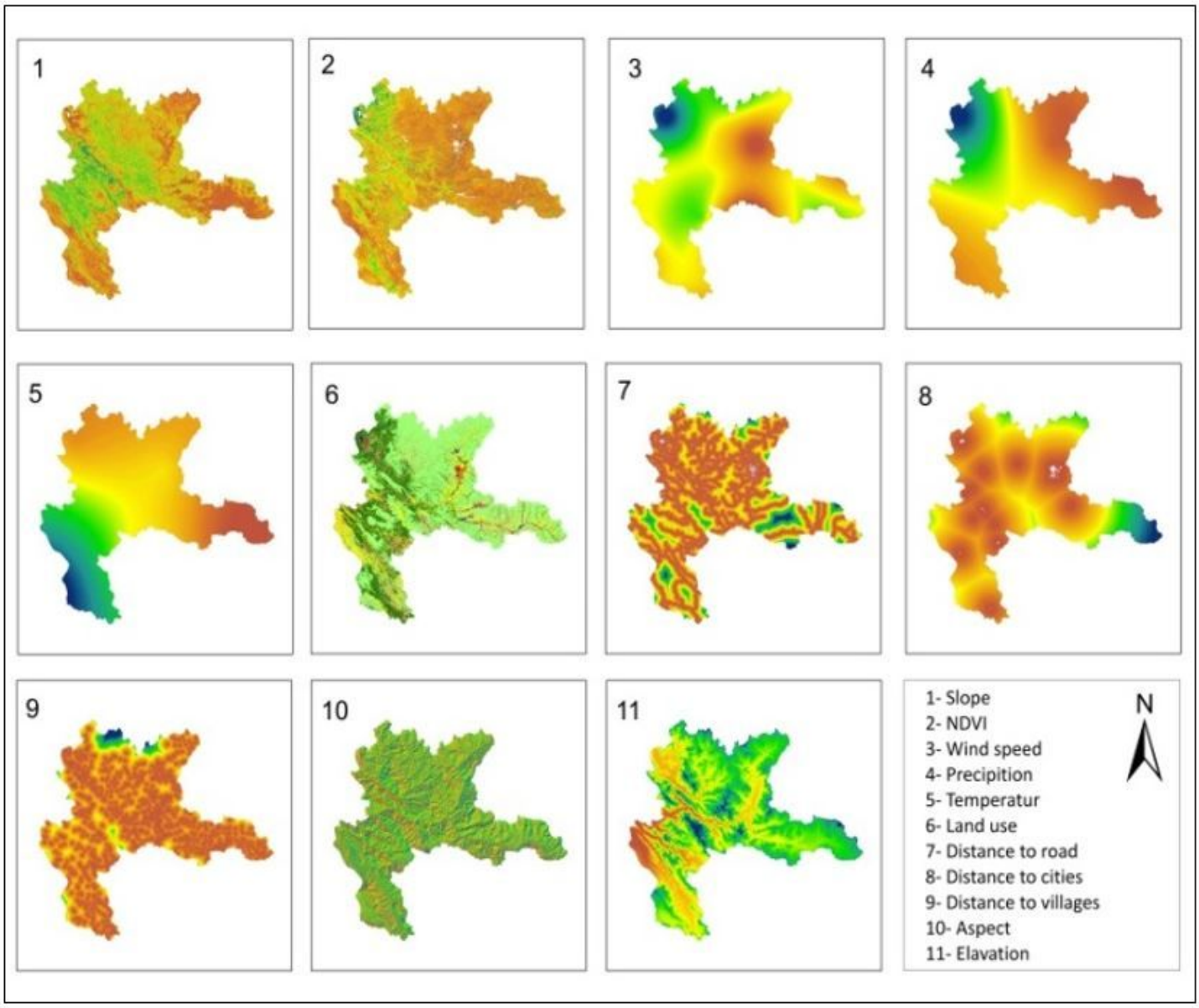

Figure 6

The fire risk factors maps applied in this study. Note: The designations employed and the presentation of the material on this map do not imply the expression of any opinion whatsoever on the part of Research Square concerning the legal status of any country, territory, city or area or of its authorities, or concerning the delimitation of its frontiers or boundaries. This map has been provided by the authors.

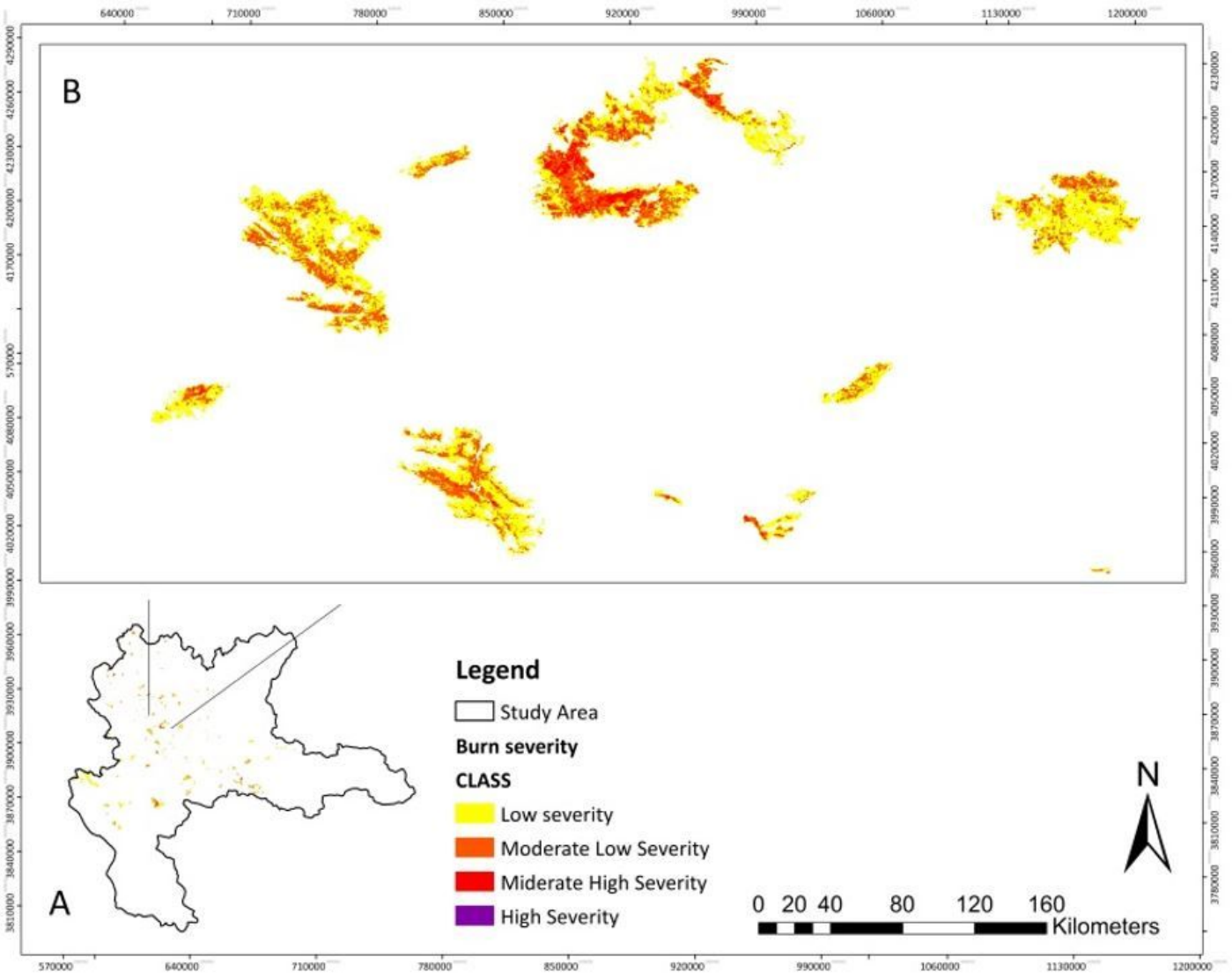

Figure 7

Fire severity of Study area. Note: The designations employed and the presentation of the material on this map do not imply the expression of any opinion whatsoever on the part of Research Square concerning the legal status of any country, territory, city or area or of its authorities, or concerning the delimitation of its frontiers or boundaries. This map has been provided by the authors.

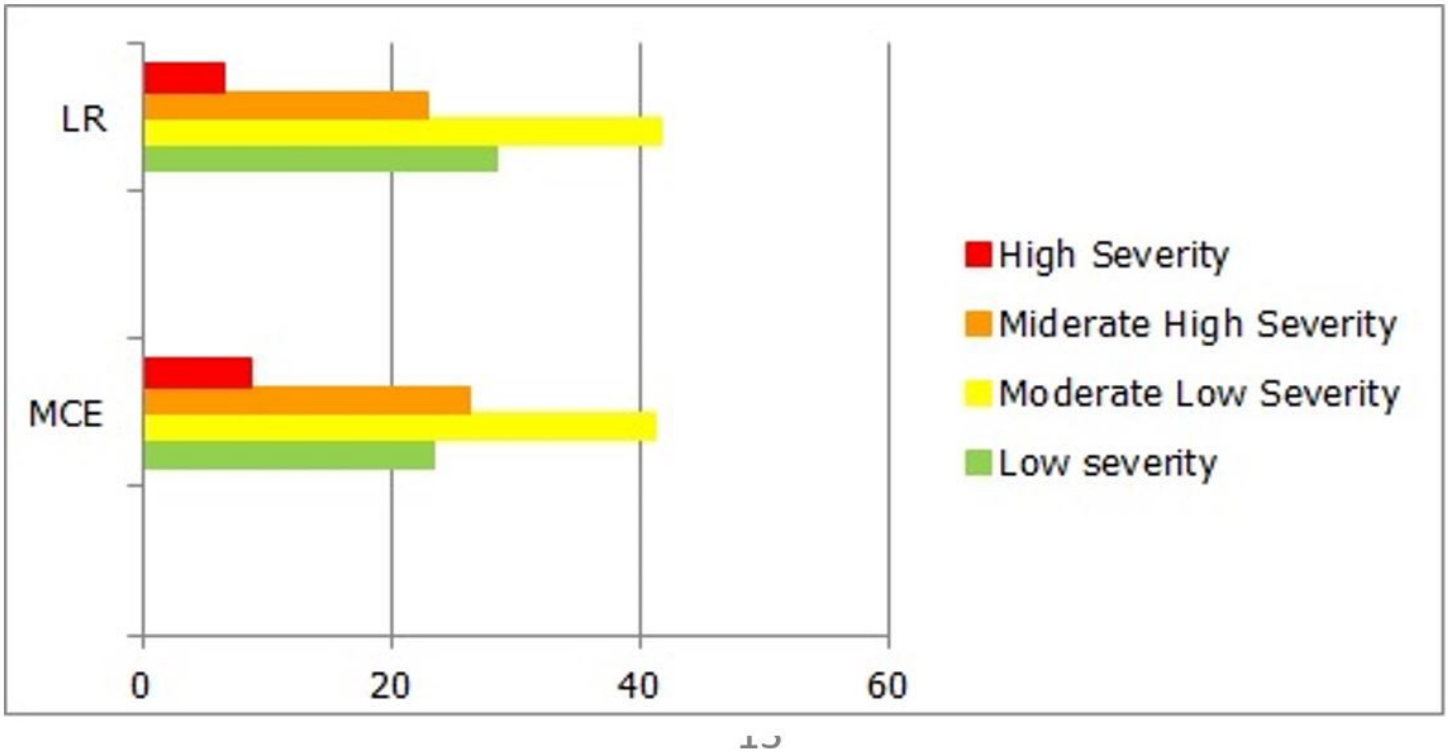

Figure 8

Percentage of classes area from probability wildfire models

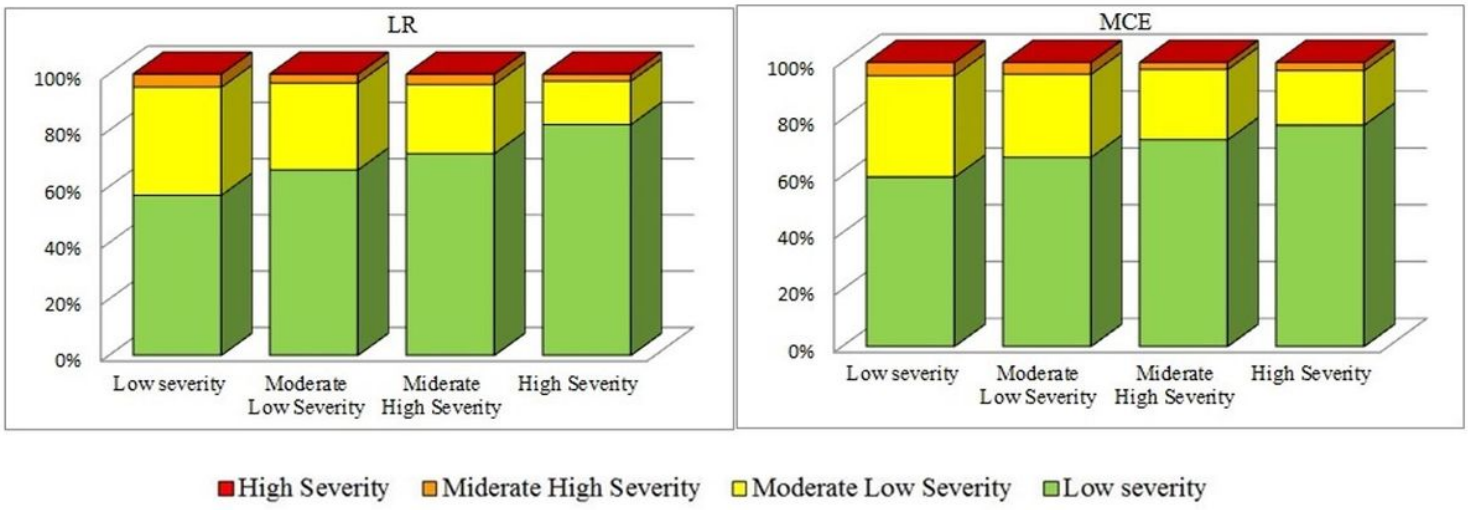

Figure 9

Comparing the class of wildfire severity in burned areas with the classes of evaluation models

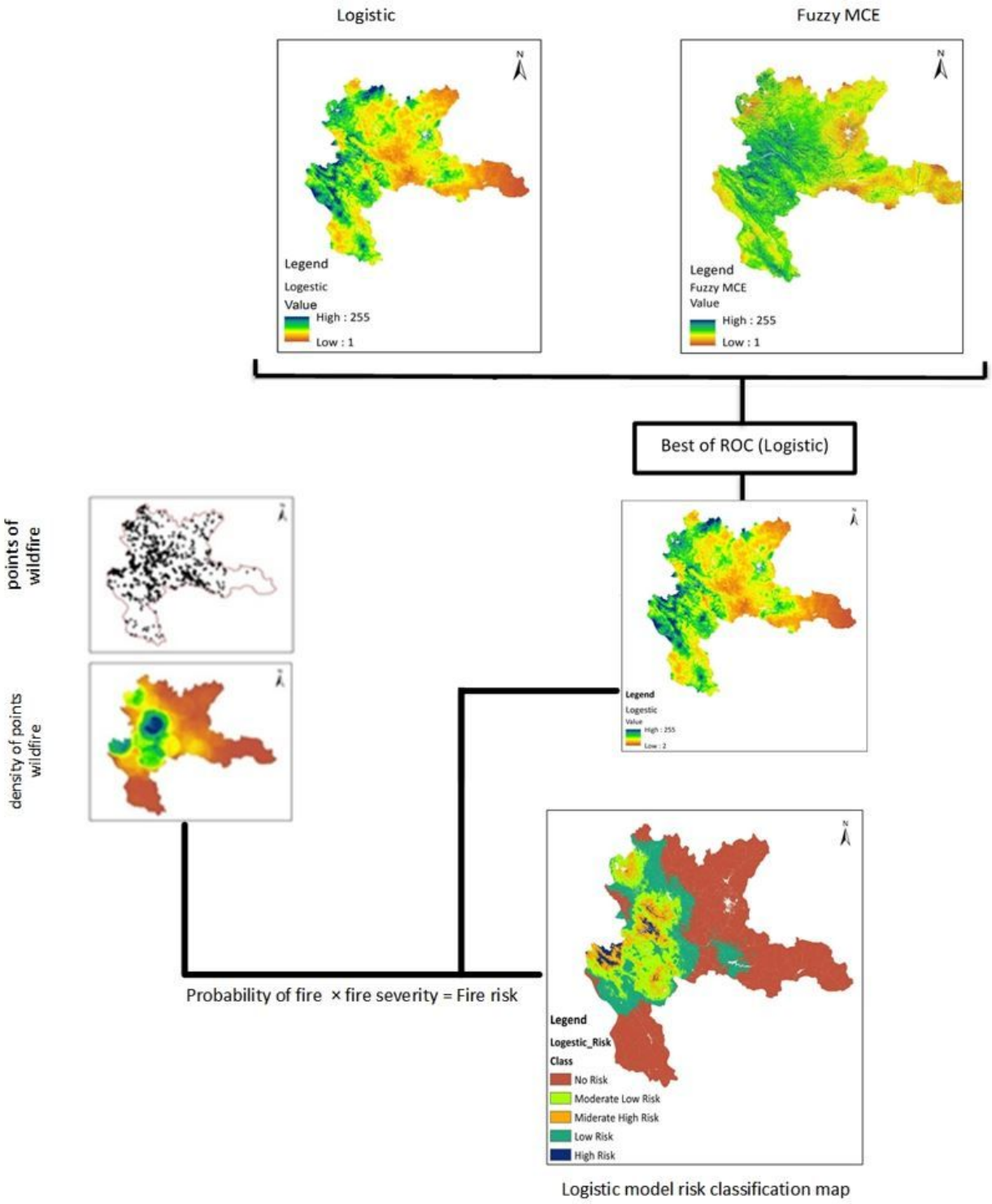

Figure 10

Framework of fire risk assessment. Note: The designations employed and the presentation of the material on this map do not imply the expression of any opinion whatsoever on the part of Research Square concerning the legal status of any country, territory, city or area or of its authorities, or concerning the delimitation of its frontiers or boundaries. This map has been provided by the authors.

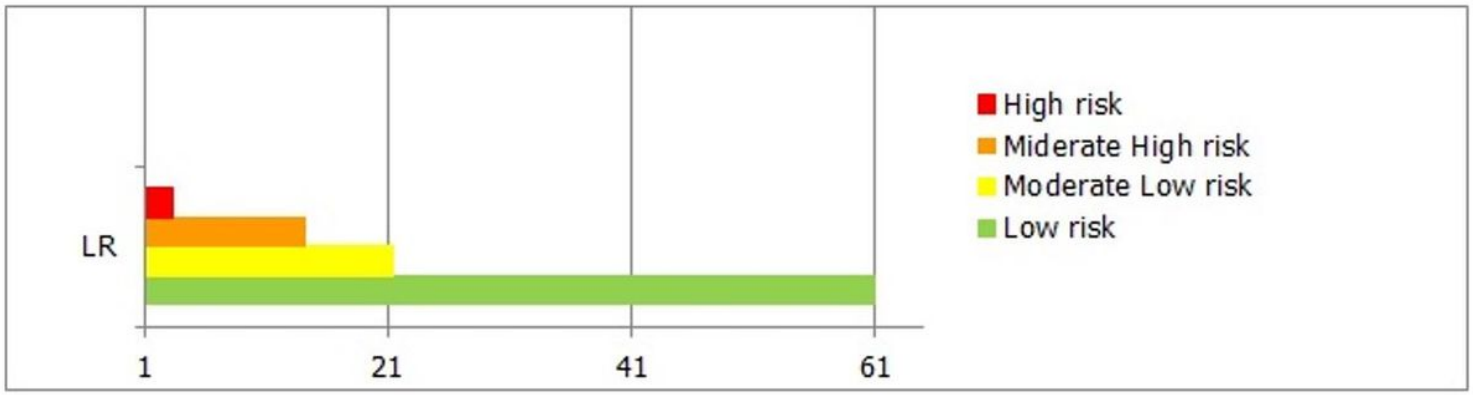

Figure 11

Percentage of classes area in fire risk models

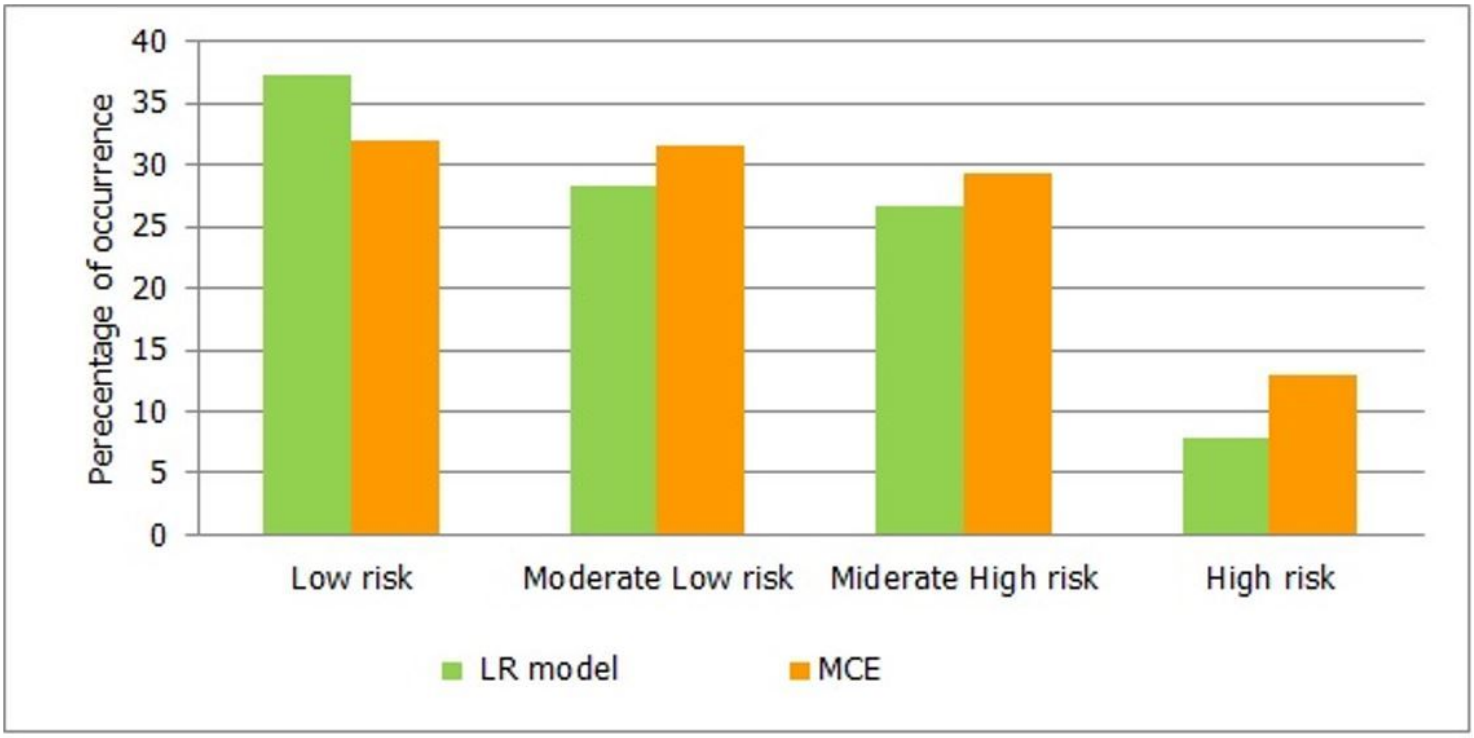

Figure 12

Percentage of wildfire occurrence according to the number of wildfires per class

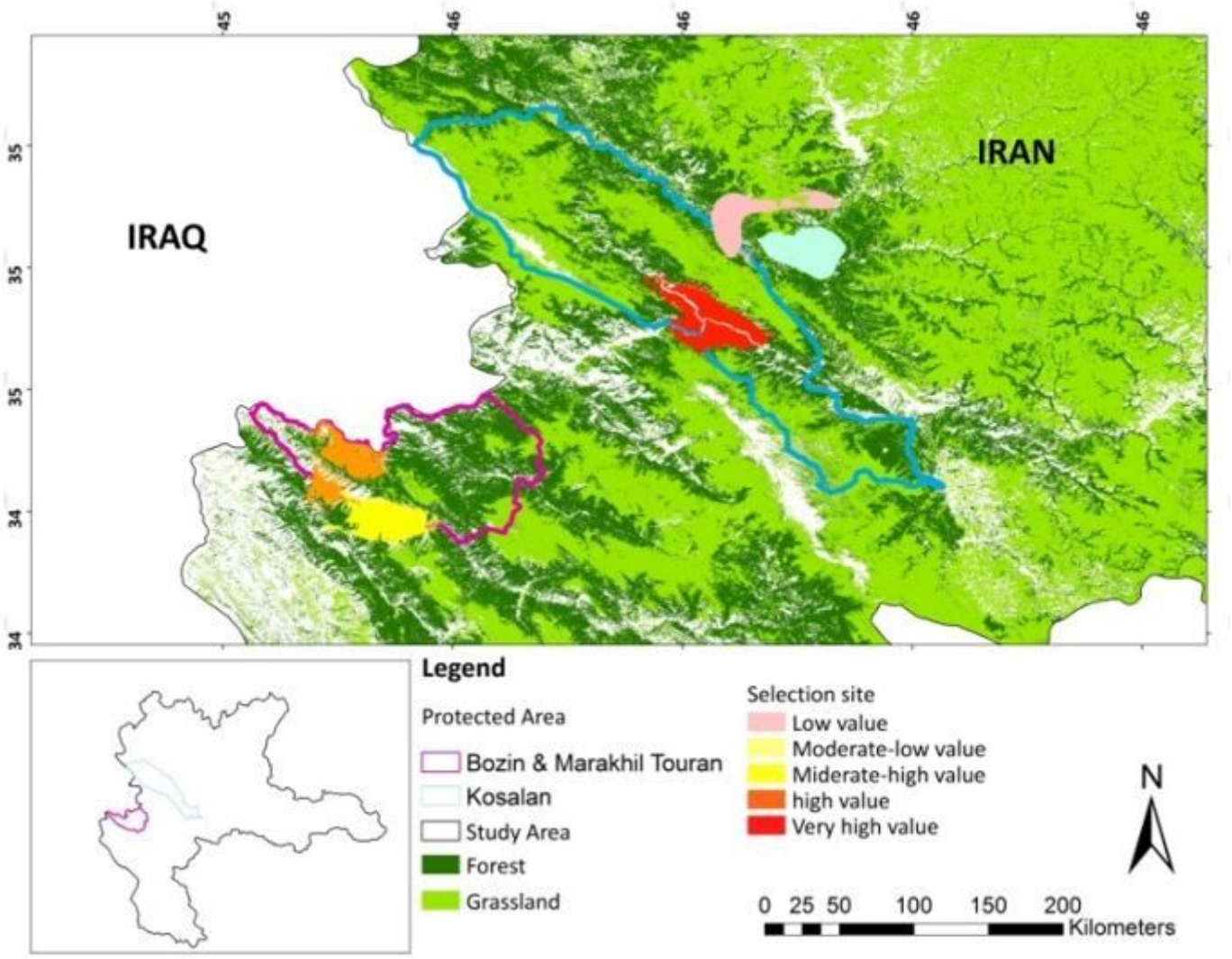

Figure 13

Selected sites as high-risk areas. Note: The designations employed and the presentation of the material on this map do not imply the expression of any opinion whatsoever on the part of Research Square concerning the legal status of any country, territory, city or area or of its authorities, or concerning the delimitation of its frontiers or boundaries. This map has been provided by the authors.

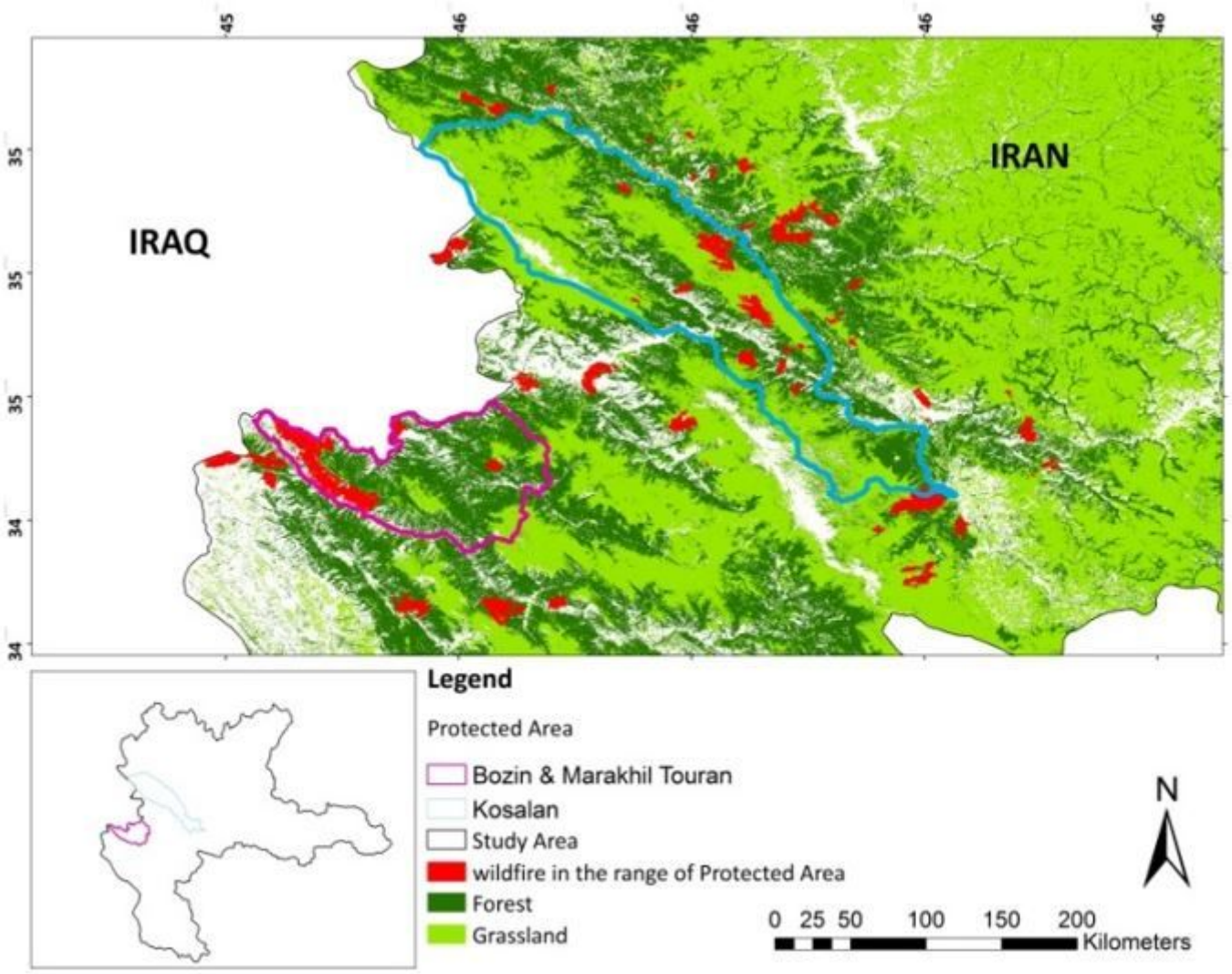

Figure 14

Wildfire in the range of protected area. Note: The designations employed and the presentation of the material on this map do not imply the expression of any opinion whatsoever on the part of Research Square concerning the legal status of any country, territory, city or area or of its authorities, or concerning the delimitation of its frontiers or boundaries. This map has been provided by the authors.

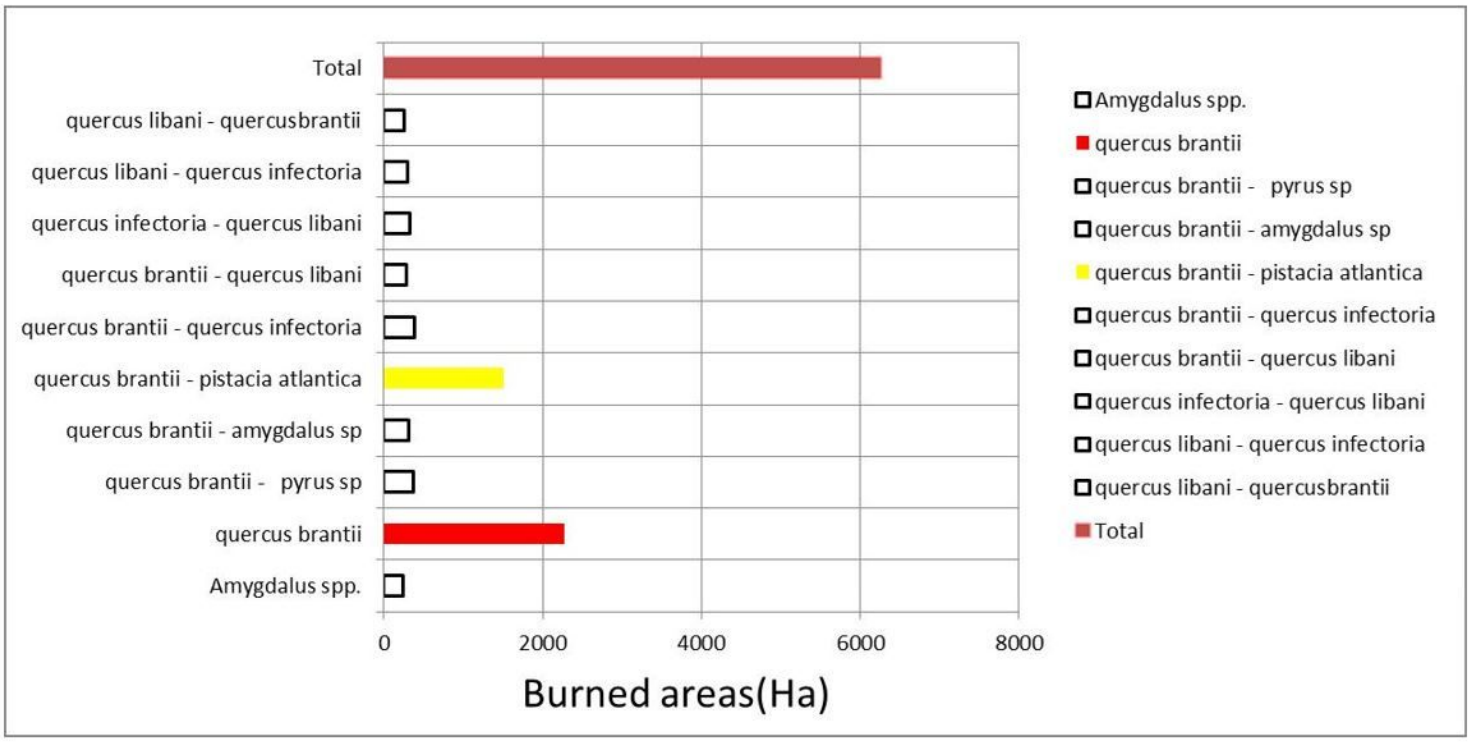

Figure 15

Forest areas burned in the study area

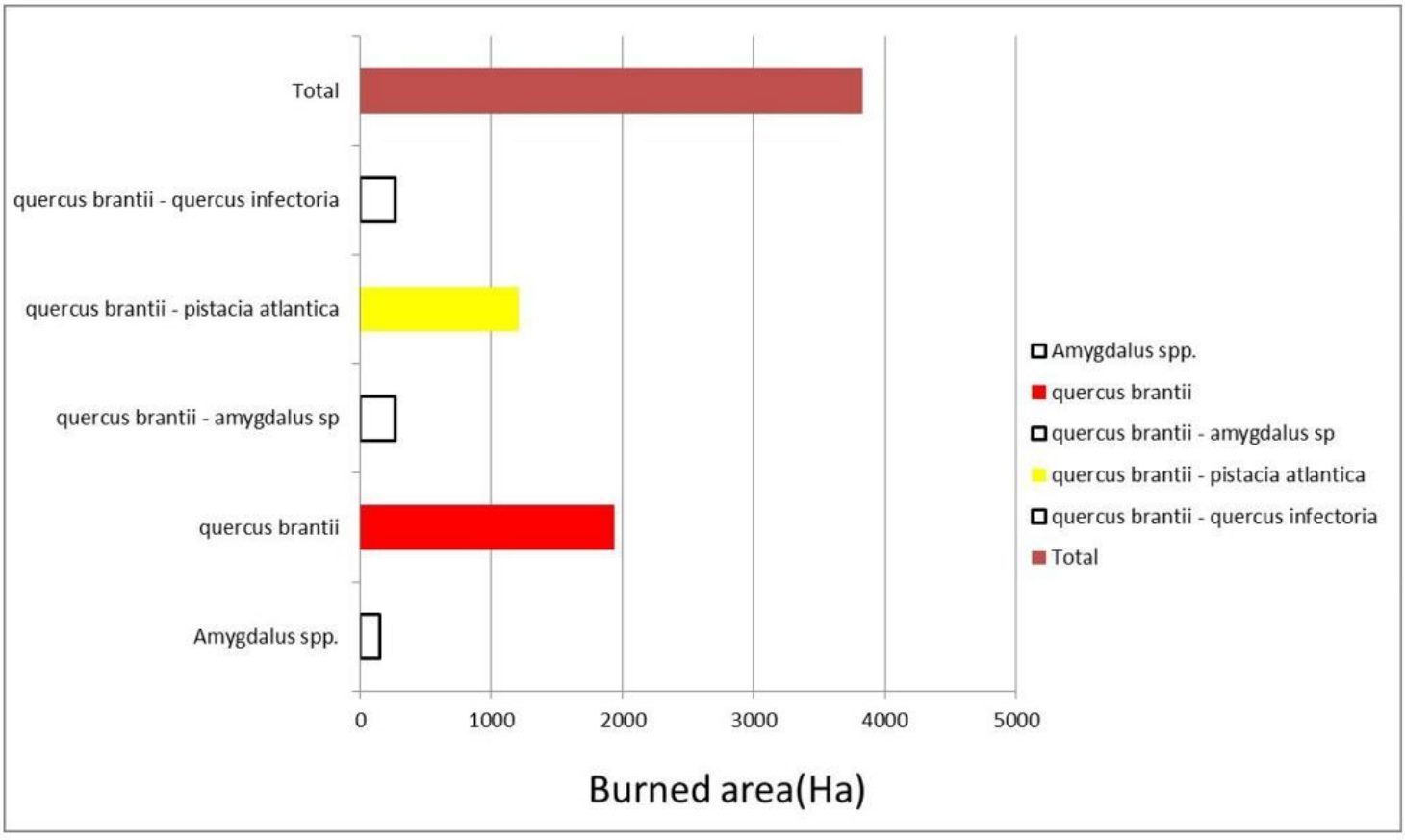

Figure 16

Forest areas burned in the range of the protected area

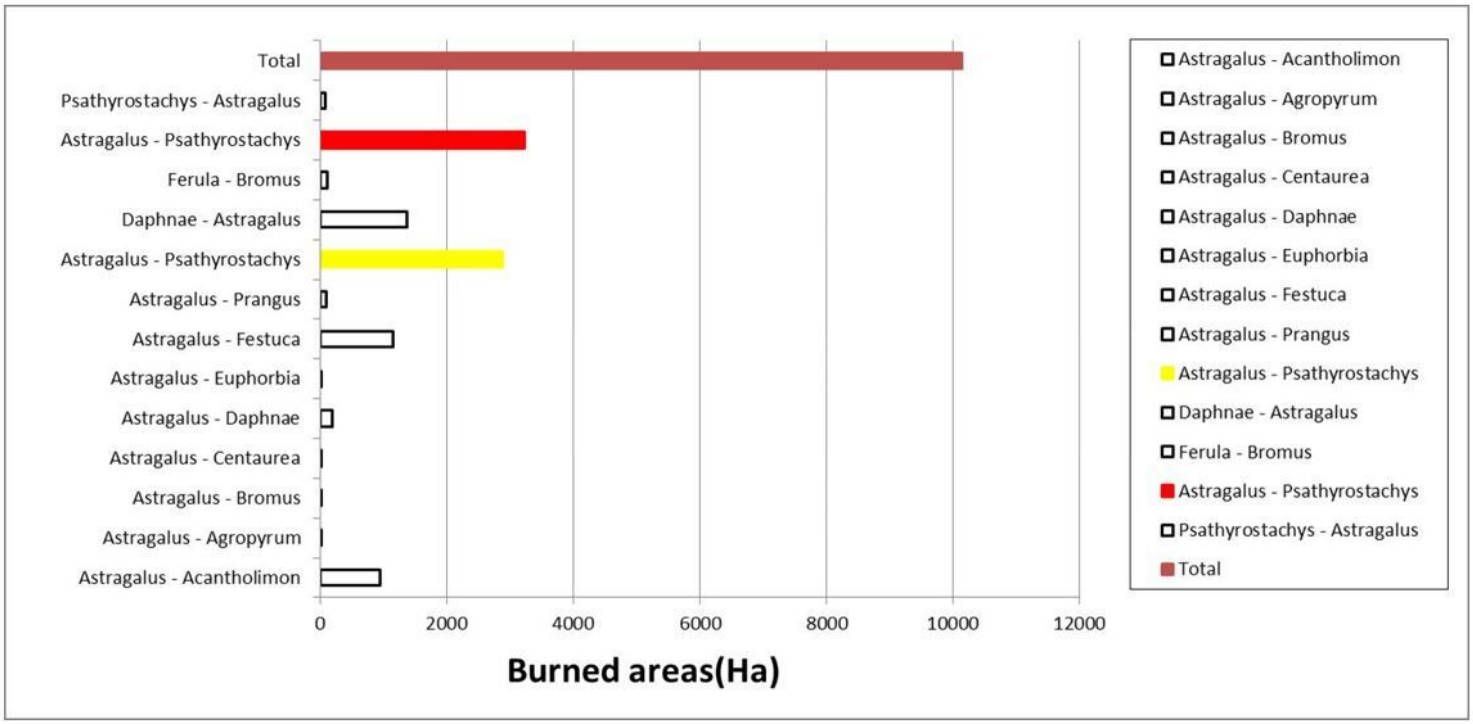

Figure 17

Rangeland areas burned in the study area

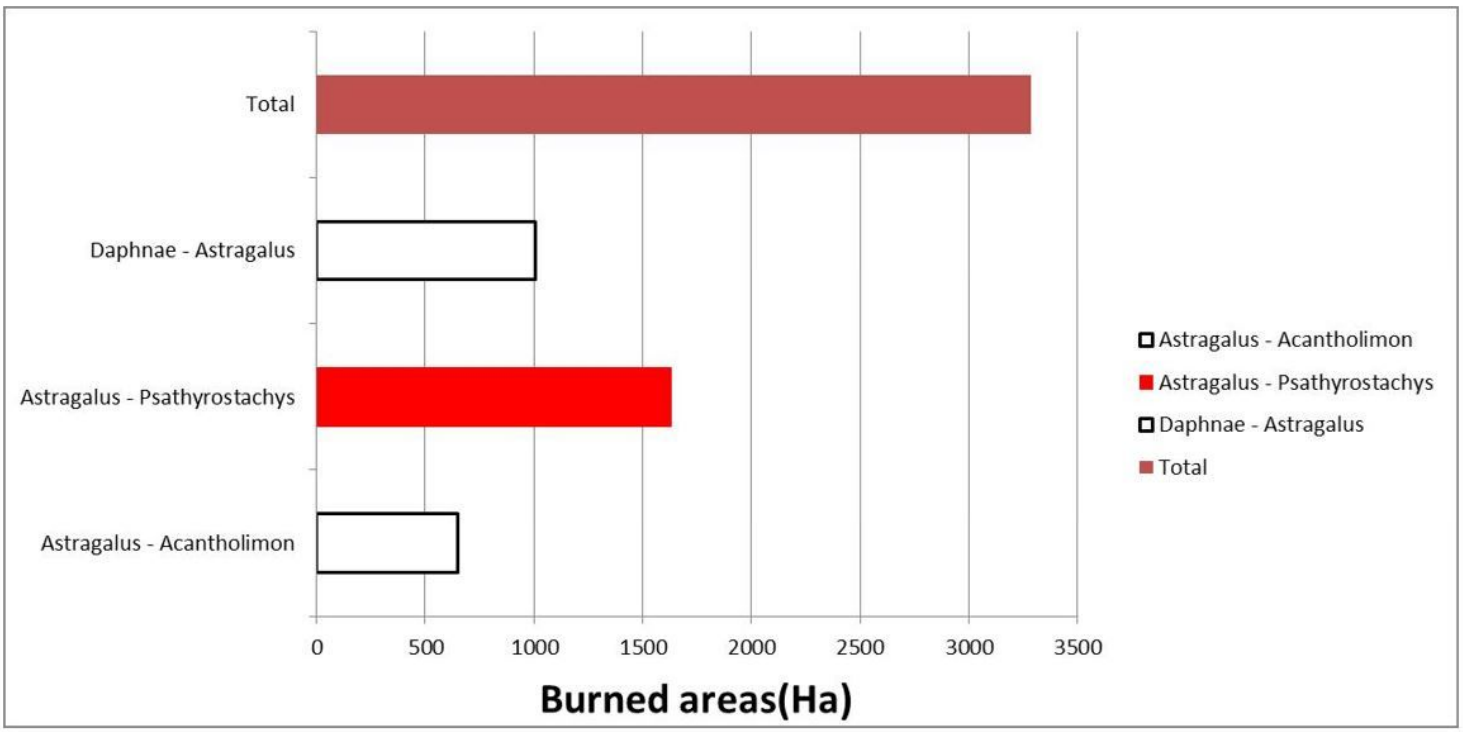

Figure 18

Rangeland areas burned in the range of the protected area